WUE-ITP-99-007
hep-ph/9904209

Constraining the Sneutrino Mass in Chargino Production and Decay with Polarized Beams

G. Moortgat-Pick, H. Fraas

Institut für Theoretische Physik, Am Hubland
D-97074 Universität Würzburg, Germany

Abstract

Production and decay of gaugino-like charginos are crucially determined by sneutrino exchange. Therefore we study the pair production of charginos $e^+e^- \to \tilde{\chi}_1^+\tilde{\chi}_1^-$ with polarized beams and the subsequent decay $\tilde{\chi}_1^- \to \tilde{\chi}_1^0 e^-\bar{\nu}_e$, including the complete spin correlations between production and decay. The spin correlations have strong influence on the decay angular distribution and on the corresponding forward–backward asymmetry. We show for two representative scenarios for $\sqrt{s} = 270$ GeV and for $\sqrt{s} = 500$ GeV that forward–backward asymmetries for polarized beams are an important tool for constraining the sneutrino mass $m_{\tilde{\nu}_e}$.

Constraining the Sneutrino Mass in Chargino Production and Decay with Polarized Beams*

G. Moortgat–Pick

and

H. Fraas

Institut für Theoret. Physik, Universität Würzburg, Am Hubland,
D-97074 Würzburg

Production and decay of gaugino-like charginos are crucially determined by sneutrino exchange. Therefore we study the pair production of charginos $e^+e^- \to \tilde{\chi}_1^+\tilde{\chi}_1^-$ with polarized beams and the subsequent decay $\tilde{\chi}_1^- \to \tilde{\chi}_1^0 e^- \bar{\nu}_e$, including the complete spin correlations between production and decay. The spin correlations have strong influence on the decay angular distribution and on the corresponding forward–backward asymmetry. We show for two representative scenarios for $\sqrt{s} = 270$ GeV and for $\sqrt{s} = 500$ GeV that forward–backward asymmetries for polarized beams are an important tool for constraining the sneutrino mass $m_{\tilde{\nu}_e}$.

PACS numbers: 12.60.Jv, 14.80.Ly, 13.88.+e, 13.10.+q, 13.30.Ce

1. Introduction

The search for supersymmetry (SUSY) is one of the main goals of the present and future colliders. In particular an e^+e^- linear collider will be an excellent discovery machine for SUSY particles [1]. Among them the charginos – mixtures of W-inos and charged higgsinos – are of particular interest. They belong to the lightest SUSY particles and are produced with large cross sections if kinematically accessible. Their properties depend on the SU(2) gaugino mass M, the higgsino mass parameter μ and the ratio $\tan\beta = v_2/v_1$ of the vacuum expectation values of the two neutral Higgs fields.

* Presented by G. Moortgat-Pick at Cracow Epiphany Conference on *Electron Positron Colliders*, Cracow, Poland, January 5–10, 1999. Work supported by the German Federal Ministry for Research and Technology (BMBF) under contract number 05 7WZ91P (0).

A number of studies addressed the determination of these fundamental SUSY parameters from chargino production at e^+e^- colliders [2, 3, 4]. Recently a procedure was proposed to determine the parameters M, μ and $\tan\beta$ independently from the decay dynamics [5]. For this, however, one has to assume that the selectron sneutrino mass $m_{\tilde{\nu}_e}$ is already known, e.g. from sneutrino pair production.

Since for gaugino-like charginos the cross section sensitively depends on the sneutrino mass the possibility to measure $m_{\tilde{\nu}_e}$ in chargino pair production at an e^+e^- collider has also been discussed [2, 4].

In this paper we study the prospects for constraining $m_{\tilde{\nu}_e}$ with suitably polarized beams by combining information from the cross section

$$\sigma_{e^-} = \sigma(e^+e^- \to \tilde{\chi}_1^+\tilde{\chi}_1^-) \times BR(\tilde{\chi}_1^- \to \tilde{\chi}_1^0 e^- \bar{\nu}_e) \tag{1}$$

and the forward–backward asymmetry (FB–asymmetry)

$$A_{FB} = \frac{\sigma_{e^-}(\cos\Theta_- > 0) - \sigma_{e^-}(\cos\Theta_- < 0)}{\sigma_{e^-}(\cos\Theta_- > 0) + \sigma_{e^-}(\cos\Theta_- < 0)} \tag{2}$$

of the decay lepton e^- from the decay $\tilde{\chi}_1^- \to \tilde{\chi}_1^0 e^- \bar{\nu}_e$. In eq.(2) Θ_- is the angle between the incoming electron beam and the outgoing e^- in the laboratory system. For constraining $m_{\tilde{\nu}}$ the simultaneous polarization of both beams turns out to be very useful [6].

In Section 2 the general formalism is presented and in Section 3 the numerical results are discussed.

2. General formalism

The production process $e^+e^- \to \tilde{\chi}_1^+\tilde{\chi}_1^-$ contains contributions from γ, Z^0 and $\tilde{\nu}_e$ exchange and the decay process, $\tilde{\chi}_1^- \to \tilde{\chi}_1^0\ell^-\bar{\nu}_e$ ($\tilde{\chi}_1^+ \to \tilde{\chi}_1^0\ell^+\nu_e$) contains contributions from W, $\tilde{\ell}_L$ and $\tilde{\nu}_e$ exchange. These processes have been studied in [7] properly taking into account the spin correlations between chargino production and decay.

In the following the amplitude for the production (decay) of $\tilde{\chi}_1^-$ with helicity λ_1 is denoted by P^{λ_1} (D_{λ_1}). All other helicity indices are suppressed. Then the amplitude of the combined process is

$$T = \Delta_{\tilde{\chi}_1^-} \sum_{\lambda_1} P^{\lambda_1} D_{\lambda_1}. \tag{3}$$

In eq. (3) $\Delta_{\tilde{\chi}_1^-} = 1/[p^2_{\tilde{\chi}_1^-} - m^2_{\tilde{\chi}_1^-} + i m_{\tilde{\chi}_1^-}\Gamma_{\tilde{\chi}_1^-}]^{-1}$, $p^2_{\tilde{\chi}_1^-}$, $m_{\tilde{\chi}_1^-}$ and $\Gamma_{\tilde{\chi}_1^-}$ denote the propagator, the four–momentum squared, the mass and the width of $\tilde{\chi}_1^-$. For this propagator we use the narrow width approximation.

The amplitude squared $|T|^2 = |\Delta_{\tilde{\chi}_1^-}|^2 \sum_{\lambda_1\lambda_1'} \rho_P^{\lambda_1\lambda_1'} \rho^D_{\lambda_1'\lambda_1}$ is thus composed of the unnormalized spin density matrix $\rho_P^{\lambda_1\lambda_1'} = P^{\lambda_1} P^{\lambda_1'*}$ of $\tilde{\chi}_1^-$ and the decay matrix $\rho^D_{\lambda_1'\lambda_1} = D_{\lambda_1} D^*_{\lambda_1'}$. Interference terms between various helicity amplitudes preclude factorization into a production factor $\sum_{\lambda_1} |P^{\lambda_1}|^2$ times a decay factor $\overline{\sum}_{\lambda_1} |D_{\lambda_1}|^2$. For the general case $e^+e^- \to \tilde{\chi}_i^+ \tilde{\chi}_j^-$ $(i,j = 1,2)$, $\tilde{\chi}_i^+ \to \tilde{\chi}_k^0 \ell^+ \nu_\ell$, $\tilde{\chi}_j^- \to \tilde{\chi}_l^0 \ell^- \bar{\nu}_\ell$ $(k,l = 1,\ldots,4)$ the complete analytical formulae for polarized beams with full spin correlations between production and decay are given in [7].

3. Numerical Results

Our study is embedded in the Minimal Supersymmetric Standard Model (MSSM) for two representative scenarios with practically the same mass of the lighter chargino and the lightest neutralino $\tilde{\chi}_1^0$, respectively. The two scenarios differ, however, significantly in the mixing character of the chargino.

The chargino mass eigenstates $\tilde{\chi}_i = \binom{\chi_i^+}{\chi_i^-}$ are defined by $\chi_i^+ = V_{i1} w^+ + V_{i2} h^+$ and $\chi_i^- = U_{i1} w^- + U_{i2} h^-$. Here $w^\pm$ and $h^\pm$ are the two-component spinor fields of the W-ino and the charged higgsinos, respectively. Furthermore U_{ij} and V_{ij} are the elements of the 2×2 matrices which diagonalize the chargino mass matrix.

Below we give the W-ino and higgsino components of the two-component spinor field χ_1^-. Similarly we give the components of the neutralino $\tilde{\chi}_1^0$ in the B-ino – W-ino basis $(\tilde{B}|\tilde{W}|\tilde{H}_a^0|\tilde{H}_b^0)$. For details see [8, 9].

Scenario A : $M = 152$ GeV, $M' = 78.7$ GeV, $\mu = 316$ GeV, $\tan\beta = 3$.

Here we have used the GUT relation $M' = \frac{5}{3} M \tan^2 \Theta_W$. This set of parameters is inspired by the low $\tan\beta$ mSUGRA reference scenario specified in [10]. The eigenstates and the masses of the lighter chargino and of the LSP $\tilde{\chi}_1^0$ are

$$\begin{aligned} \chi_1^- &= (-0.91| + 0.42) \quad \text{and} \quad m_{\tilde{\chi}_1^-} = 128 \text{ GeV}, \\ \tilde{\chi}_1^0 &= (-0.97| + 0.15| - 0.15| - 0.15) \quad \text{and} \quad m_{\tilde{\chi}_1^0} = 71 \text{ GeV}. \end{aligned}$$

Scenario B : $M = 400$ GeV, $M' = 95$ GeV, $\mu = 145$ GeV, $\tan\beta = 3$.

Here the parameters are chosen thus that the chargino is higgsino-like with only a small gaugino component. To obtain nearly the same masses as in

Scenario A and an as large as possible higgsino component for $\tilde{\chi}_1^0$ we take M and M' as independent parameters and do not use the GUT relation between them. The eigenstates and masses are

$$\chi_1^- = (-0.19| + 0.98) \quad \text{and} \quad m_{\tilde{\chi}_1^-} = 129 \text{ GeV},$$
$$\tilde{\chi}_1^0 = (-0.82| + 0.11| - 0.45| - 0.33) \quad \text{and} \quad m_{\tilde{\chi}_1^0} = 71 \text{ GeV}.$$

In both scenarios the LSP $\tilde{\chi}_1^0$ has a dominating B-ino component.

We vary the sneutrino mass $m_{\tilde{\nu}_e}$ between 80 GeV and 1000 GeV. The mass of the left selectron $m_{\tilde{e}_L}$ is determined by the relation

$$m_{\tilde{e}_L}^2 - m_{\tilde{\nu}_e}^2 = -M_W^2 \cos 2\beta. \tag{4}$$

This sum rule is independent of any assumption about the gaugino mass parameters and on the assumption of a universal scalar mass m_0 [11].

The influence of spin correlations between production and decay on the decay angular distributions is strongest near threshold. Therefore numerical results are presented for energies near threshold $\sqrt{s} = 270$ GeV and for $\sqrt{s} = 500$ GeV.

We have calculated for longitudinally polarized beams the cross section σ_{e^-}, eq. (1), and the FB–asymmetry A_{FB}, eq. (2), of the decay electron. For the polarization of the e^- beam we assume $P_- = \pm 85\%$ and for the polarization of the e^+ beam we take $P_+ = \pm 60\%$. Simultaneous polarization of both beams is not only useful to enlarge σ_{e^-} but it can also have strong influence on A_{FB} according to the mixing character of the charginos. Since the sneutrino couples only to left-handed electrons the polarization $P_- < 0$ ($P_+ > 0$) for the $e^-(e^+)$ beam is favourable for studying its properties.

3.1. Cross sections

For the gaugino-like scenario A and $\sqrt{s} = 270$ GeV the cross section σ_{e^-} is shown in Fig. 1. For $m_{\tilde{\nu}_e}$ between 80 GeV and 400 GeV it is very sensitive on $m_{\tilde{\nu}_e}$. The deep dip at $m_{\tilde{\nu}_e} \approx 130$ GeV is due to the destructive interferences between gauge boson and slepton exchange [9, 12]. For $m_{\tilde{\nu}_e} < m_{\tilde{\chi}_1^-}$ the cross section increases owing to the two-body decay $\tilde{\chi}_1^- \to \tilde{\nu}_e e^-$. However, for $\sqrt{s} = 270$ GeV this effect is suppressed by destructive interference effects.

For higher energy $\sqrt{s} = 500$ GeV, Fig. 2, the destructive Z^0–$\tilde{\nu}_e$ interference in production is shifted to higher $m_{\tilde{\nu}_e}$ and the two-body decay

threshold is more apparent. For values of $m_{\tilde{\nu}_e} > 200$ GeV the cross section σ_{e^-} for $\sqrt{s} = 500$ GeV is smaller than for $\sqrt{s} = 270$ GeV.

Beam polarization has strong influence on the magnitude of σ_{e^-}. For $P_- = -85\%$ and $P_+ = +60\%$ it increases by a factor of about 3, nearly independent of $\sqrt{s}$ and of $m_{\tilde{\nu}_e}$, Fig. 1 and Fig. 2. For the opposite polarization configuration, $P_- = +85\%, P_+ = -60\%$, it would decrease by a factor of 0.06. If only the electron beam is polarized σ_{e^-} increases for $P_- = -85\%$ by a factor of 1.85 and for $P_- = +85\%$ it decreases by a factor of 0.15.

In Fig. 3 and Fig. 4 we show σ_{e^-} for the higgsino-like scenario B. Since the dominating higgsino components do not couple to sneutrinos, the small gaugino admixture causes only a weak dependence on $m_{\tilde{\nu}_e}$, Fig. 3. The destructive interference between Z^0 and $\tilde{\nu}_e$ exchange is suppressed by the dominating higgsino component. For $m_{\tilde{\nu}_e} > m_{\tilde{\chi}_1^-}$ the cross section is practically independent of $m_{\tilde{\nu}_e}$. Only for $m_{\tilde{\nu}_e} < m_{\tilde{\chi}_1^-}$ it shows a strong dependence on the sneutrino mass due to the two-body decay $\tilde{\chi}_1^- \to \tilde{\nu}_e e^-$.

For higher energy, $\sqrt{s} = 500$ GeV, Fig. 4, σ_{e^-} is smaller. The dependence on $m_{\tilde{\nu}_e}$, however, is essentially unchanged.

Also for higgsino-like charginos beam polarization has a strong influence on the magnitude of σ_{e^-}. For $P_- = -85\%$ and $P_+ = +60\%$ and for both values of $\sqrt{s}$, Fig. 3 and Fig. 4, σ_{e^-} increases by a factor of about 2.5, which is somewhat smaller as for the gaugino-like scenario A. For the opposite polarization, $P_- = +85\%, P_+ = -60\%$, σ_{e^-} decreases by a factor of 0.5. If only the e^- beam is polarized with $P_- = -85\%(P_- = +85\%)$ the cross section increases(decreases) by a factor of 1.6(0.4).

3.2. Forward–backward asymmetry of the decay lepton

In this section we study the FB–asymmetry A_{FB} of the decay electron, eq. (2), for $m_{\tilde{\nu}_e}$ between 80 GeV and 1000 GeV. Since the angular distribution of the chargino decay products is determined by the polarization of the decaying chargino, the FB–asymmetry of the decay lepton strongly depends on the spin correlations between production and decay. The dependence of A_{FB} on $m_{\tilde{\nu}_e}$, on the beam polarization and on $\sqrt{s}$ is a result of the complex interplay between production and decay.

In scenario A for $\sqrt{s} = 270$ GeV the dependence of A_{FB} on $m_{\tilde{\nu}_e}$ is shown in Fig. 5. For high $m_{\tilde{\nu}_e} > 400$ GeV it is about 8% and is nearly independent of $m_{\tilde{\nu}_e}$. For $m_{\tilde{\nu}_e} < 400$ GeV, however, A_{FB} shows a complex and interesting mass dependence. The destructive Z^0–$\tilde{\nu}_e$ interference in the production causes large $A_{FB} \approx 30\%$. Since this destructive interference effect vanishes at about $m_{\tilde{\nu}_e} \approx 200$ GeV the FB–asymmetry decreases for higher values

of $m_{\tilde{\nu}_e}$. The deep dip at $m_{\tilde{\nu}_e} \approx 140$ GeV is due to destructive W–$\tilde{\nu}_e$ (W–$\tilde{e}$) interference in the decay process $\tilde{\chi}_1^- \to \tilde{\chi}_1^0 e^- \bar{\nu}_e$. For $m_{\tilde{\nu}_e} \leq m_{\tilde{\chi}_1^-}$ the FB–asymmetry strongly increases up to about 35%, owing to the two-body decay $\tilde{\chi}_1^- \to \tilde{\nu}_e e^-$.

For $\sqrt{s} = 500$ GeV, Fig. 6, large values of A_{FB} up to 50% can be reached in scenario A. The Z^0–$\tilde{\nu}_e$ interference effect in production is shifted to higher $m_{\tilde{\nu}_e}$ so that just for $m_{\tilde{\nu}_e} \geq 250$ GeV A_{FB} decreases from 48% to 10% for $m_{\tilde{\nu}_e} = 1000$ GeV. For $\sqrt{s} = 500$ GeV the Z^0–$\tilde{\nu}_e$ interference in the decay process is less important because for higher energies the characteristics of the production process is more and more dominating. Therefore at $m_{\tilde{\nu}_e} \approx 140$ GeV A_{FB} decreases only to about 43% in contrast to the deep dip at $m_{\tilde{\nu}_e} \approx 140$ GeV for $\sqrt{s} = 270$ GeV. Again, for $m_{\tilde{\nu}_e} \leq m_{\tilde{\chi}_1^-}$ the two-body decay $\tilde{\chi}_1^- \to \tilde{\nu}_e e^-$ involves large $A_{FB} \approx 50\%$.

Note that in the gaugino-like scenario A A_{FB} is nearly independent on beam polarization. This emerges as a consequence of the fact that in scenario A the beam polarization changes the magnitude of σ_{e^-} by a factor which is nearly independent of $m_{\tilde{\nu}_e}$. This factor cancels in A_{FB}, eq. (2). Only for $P_- > 0$ a small polarization effect can be observed, see Fig. 5 and Fig. 6.

In the higgsino-like scenario B, Fig. 7, the FB–asymmetry for $\sqrt{s} = 270$ GeV is much smaller than in scenario A, $A_{FB} \approx 5\%$ for $m_{\tilde{\nu}_e} \geq m_{\tilde{\chi}_1^-}$. Only for $m_{\tilde{\nu}_e} \leq m_{\tilde{\chi}_1^-}$ when the two-body decay $\tilde{\chi}_1^- \to e^- \tilde{\nu}_e$ is open large $A_{FB} \approx 33\%$ can be reached for unpolarized beams.

For $\sqrt{s} = 500$ GeV A_{FB} decreases, $A_{FB} \leq 5\%$ for $m_{\tilde{\nu}_e} \geq m_{\tilde{\chi}_1^-}$ and $A_{FB} \approx 18\%$ for $m_{\tilde{\nu}_e} \leq m_{\tilde{\chi}_1^-}$, Fig. 8.

In this higgsino-like scenario B the FB–asymmetry sensitively depends on the beam polarization. For $P_- = -85\%, P_+ = +60\%$ the FB–asymmetry increases for $m_{\tilde{\nu}_e} \leq m_{\tilde{\chi}_1^-}$ up to 48% for $\sqrt{s} = 270$ GeV and up to 28% for $\sqrt{s} = 500$ GeV. If only the electron beam is polarized with $P_- = +85\%$, one even obtains for $m_{\tilde{\nu}_e} \leq m_{\tilde{\chi}_1^-}$ large negative FB–asymmetries, $A_{FB} \approx -20\%(A_{FB} \approx -12\%)$, for $\sqrt{s} = 270$ GeV$(\sqrt{s} = 500$ GeV).

3.3. Constraining $m_{\tilde{\nu}_e}$

In this section we study the prospects to constrain $m_{\tilde{\nu}_e}$ by measuring σ_{e^-} and A_{FB} with different beam polarizations.

We assume that $\tan\beta$, $m_{\tilde{\chi}_1^-}$ and $m_{\tilde{\chi}_1^0}$ are already known and we choose as an example the gaugino-like scenario A and the higgsino-like scenario B.

One obtains the largest cross sections for polarizations $P_- < 0$, $P_+ > 0$. We therefore assume that σ_{e^-} has been measured for beam polarizations $P_- = -85\%$, $P_+ = +60\%$ and for energies $\sqrt{s} = 270$ GeV and $\sqrt{s} = 500$ GeV with an error of 5%. We study also the correponding A_{FB} for two combinations of beam polarizations, $P_- = -85\%$, $P_+ = +60\%$ and $P_- = +85\%, P_+ = 0\%$. For the second case we use unpolarized positrons since also switching the e^+ polarization gives extremely small rates.

3.3.1. Constraining $m_{\tilde{\nu}_e}$ for $\sqrt{s} = 270$ GeV

We assume that for $\sqrt{s} = 270$ GeV and $P_- = -85\%$, $P_+ = +60\%$ a cross section of $\sigma_{e^-} = 180fb \pm 5\%$ has been measured. As can be seen from Fig. 1 for scenario A and from Fig. 3 for scenario B this cross section is compatible with two regions for $m_{\tilde{\nu}_e}$ in either case.

In scenario A the cross section is compatible with small values of $m_{\tilde{\nu}_e}$ between 85 GeV and 89 GeV and with high $m_{\tilde{\nu}_e}$ between 240 GeV and 255 GeV, Fig. 1. For the case of low $m_{\tilde{\nu}_e}$ the FB–asymmetry is between 29% and 32% and for high $m_{\tilde{\nu}_e}$ between 19% and 22%, Fig. 5. Accordingly A_{FB} allows to discriminate between the two regions for $m_{\tilde{\nu}_e}$. Changing the polarization to $P_- = +85\%$, $P_+ = 0\%$, the FB–asymmetry gives no additional constraints for $m_{\tilde{\nu}_e}$, Fig. 5.

In scenario B the cross section is compatible with small $m_{\tilde{\nu}_e}$ between 128 GeV and 140 GeV near the two-body decay threshold and with high $m_{\tilde{\nu}_e} > 250$ GeV, Fig. 3. For the case of low $m_{\tilde{\nu}_e}$ the FB–asymmetry is between 11% and 29% and for high $m_{\tilde{\nu}_e}$ A_{FB} is less than 5%, Fig. 7. Again A_{FB} allows to discriminate between the two regions for $m_{\tilde{\nu}_e}$.

In our examples with $P_- = -85\%$, $P_+ = +60\%$ the values of the FB–asymmetry for the low mass region of scenario B (11%–29%) overlaps with that for the low mass region of scenario A (29%–32%) as well as with that of the high mass region of scenario A (19%–22%).

However measuring A_{FB} for a suitably polarized electron beam and an unpolarized positron beam allows to discriminate between scenario A and scenario B. For $P_- = +85\%$, $P_+ = 0\%$ the FB–asymmetry in the low mass region of scenario B is negative between -5% and -16%, whereas for scenario A the respective regions for A_{FB} are unchanged, compare Fig. 5 and Fig. 7.

3.3.2. Constraining $m_{\tilde{\nu}_e}$ for $\sqrt{s} = 500$ GeV

In the same manner we study σ_{e^-} and A_{FB} for $\sqrt{s} = 500$ GeV. We assume that for polarized beams with $P_- = -85\%$, $P_+ = +60\%$ the cross section $\sigma_{e^-} = 130fb \pm 5\%$ has been measured. As can be seen from Fig. 2 for scenario A and Fig. 4 for scenario B this cross section is again compatible with two regions for $m_{\tilde{\nu}_e}$ in either case.

In scenario A σ_{e^-} is compatible with small values of $m_{\tilde{\nu}_e}$ between 161 GeV and 175 GeV and with high values of $m_{\tilde{\nu}_e}$ between 420 GeV and 450 GeV, Fig. 2. For small $m_{\tilde{\nu}_e}$ the FB–asymmetry is about 45% whereas for high $m_{\tilde{\nu}_e}$ it is between 32% and 35%, clearly distinguishable from the case of low $m_{\tilde{\nu}_e}$, Fig. 6. As compared to the case of lower energies, $\sqrt{s} = 270$ GeV, the values of A_{FB} are higher and restricted to smaller regions. Changing the beam polarization to $P_- = +85\%$, $P_+ = 0\%$ the FB–asymmetry gives practically no additional constraints for $m_{\tilde{\nu}_e}$, Fig. 6.

In scenario B σ_{e^-} is compatible with small $m_{\tilde{\nu}_e}$ in the region between 122 GeV and 128 GeV near the two-body decay threshold and with high $m_{\tilde{\nu}_e} > 750$ GeV, Fig. 4. For low $m_{\tilde{\nu}_e}$ the FB–asymmetry is between 10% and 28% whereas for high values of $m_{\tilde{\nu}_e}$ it is rather small, $A_{FB} < 3\%$. These two regions for $m_{\tilde{\nu}_e}$ can clearly be distinguished by measuring A_{FB}, Fig. 8.

Similar as for lower energies, $\sqrt{s} = 270$ GeV, the regions for A_{FB} for the case of high $m_{\tilde{\nu}_e}$ in scenario A and for the case of $m_{\tilde{\nu}_e} \approx m_{\tilde{\chi}_1^-}$ in scenario B are not well separated. Again a suitably polarized e^- beam and an unpolarized e^+ beam allow to discriminate between scenario A and scenario B. For $P_- = +85\%$, $P_+ = 0\%$ the FB–asymmetry is negative between $A_{FB} = -8\%$ and $A_{FB} = -12\%$ in scenario B, whereas it has large positive values between $A_{FB} = 31\%$ and $A_{FB} = 34\%$ in scenario A, compare Fig. 6 and Fig. 8.

4. Summary and Conclusions

For the determination of the MSSM parameters M, μ and $\tan\beta$ from chargino production, the sneutrino mass plays a crucial role. With regard to the determination of the sneutrino mass we have studied chargino pair production $e^+e^- \to \tilde{\chi}_1^+\tilde{\chi}_1^-$ with polarized beams and the subsequent leptonic decay $\tilde{\chi}_1^- \to \tilde{\chi}_1^0 e^- \bar{\nu}_e$ taking into account the complete spin correlations between production and decay. The spin correlations are crucial for the decay angular distributions and on the forward–backward asymmetries of the decay leptons.

We have presented a method for constraining $m_{\tilde{\nu}_e}$ if $\tan\beta$ and the masses of $\tilde{\chi}_1^-$ and of $\tilde{\chi}_1^0$ are known. Accordingly we choose two representative scenarios with a dominating gaugino and with a dominating higgsino component of $\tilde{\chi}_1^-$, respectively. We have studied the prospect to constrain the sneutrino mass by measuring polarized cross sections and FB–asymmetries of the decay leptons in the laboratory system.

Simultaneous polarization of both beams is not only important for enlarging the cross section but it can also have rather strong influence on the FB–asymmetry of the decay electron depending on the mixing char-

acter of the charginos. For charginos with dominating gaugino character the FB–asymmetry is practically inpendent of the beam polarization. But for higgsino-like charginos beam polarization can considerably influence the FB–asymmetry.

In our examples σ_{e^-} measured for the beam polarization $P_- = -85\%$, $P_+ = +60\%$ with an error of 5%, e.g., is compatible with two regions for $m_{\tilde{\nu}_e}$. For gaugino-like charginos as well as for higgsino-like ones the corresponding FB–asymmetry allows to distinguish between the two regions of $m_{\tilde{\nu}_e}$. Beyond that the two mixing scenarios can be distinguished by additional measurement of the FB–asymmetry with a right polarized e^- beam. Then the sign of A_{FB} changes for higgsino-like charginos.

We have presented numerical results for $\sqrt{s} = 270$ GeV, near the chargino production threshold, and for $\sqrt{s} = 500$ GeV. For gaugino-like charginos $m_{\tilde{\nu}_e}$ can be constrained up to a few GeV, for higgsino-like charginos this is possible if $m_{\tilde{\nu}_e}$ is in the vicinity of the chargino mass. Obviously a complete MC study with inclusion of experimental cuts would be indispensable for realistic predictions.

G. M.–P. thanks M. Jezabek and the other organizers of the Epiphany Conference for the extremely hostly and friendly atmosphere during the Conference. We are grateful to V. Latussek for his support in the development of the numerical program. G.M.–P. was supported by *Stiftung für Deutsch–Polnische Zusammenarbeit* and by *Friedrich–Ebert–Stiftung*.

REFERENCES

[1] JLC Group, JLC-1, KEK Report No. 92-16 (1992);
DESY-Reports, DESY 92-123 A,B; DESY 93-123 C; DESY 96-123 D; DESY 97-123 E; Phys. Rept. **299** (1998) 1;
SLAC-Report 485, submitted to Snowmass 1996.

[2] J.L. Feng, M.J. Strassler, Phys. Rev. **D 51** (1995) 4661;
J.L. Feng, M.J, Strassler, Phys. Rev. **D 55** (1997) 1326;
J.L Feng, M.E. Peskin, H. Murayama, X. Tata, Phys.Rev. **D 52** (1995) 1418.

[3] G. Moultaka, hep-ph/9810214;
V. Lafage, T. Ishikawa, T. Kaneko, T. Kon, Y. Kurihara, H. Tanaka, hep-ph/9810504.

[4] T. Tsukamoto, K. Fujii, H. Murayama, M. Yamaguchi, Y. Okada, Phys. Rev. **D 51** (1995) 3153.

[5] S.Y. Choi, A. Djouadi, H. Dreiner, J. Kalinowski, P. Zerwas, Eur. Phys. J. **C 7** (1999) 123;
S.Y. Choi, A. Djouadi, H.S. Song, P. Zerwas, hep-ph/9812236.

[6] G. Moortgat–Pick, H. Fraas, A. Bartl, W. Majerotto, Act. Phys. Pol. **B 29** (1998) 1497.

[7] G. Moortgat–Pick, H. Fraas, A. Bartl, W. Majerotto, Eur. Phys. J. **C 7** (1999) 113.

[8] H.E. Haber, G.L. Kane, Phys. Rep. **117** (1985) 75.

[9] A. Bartl, H. Fraas, W. Majerotto, Z. Phys. **C 30**, (1986) 441.

[10] S. Ambrosanio, G.A. Blair, P. Zerwas, ECFA-DESY LC-Workshop, 1998.

[11] S.P. Martin, P. Ramond, Phys. Rev. **D 48** (1993) 5365.

[12] A. Bartl, H. Fraas, W. Majerotto, B. Mösslacher, Z. Phys. **C 55** (1992) 257.

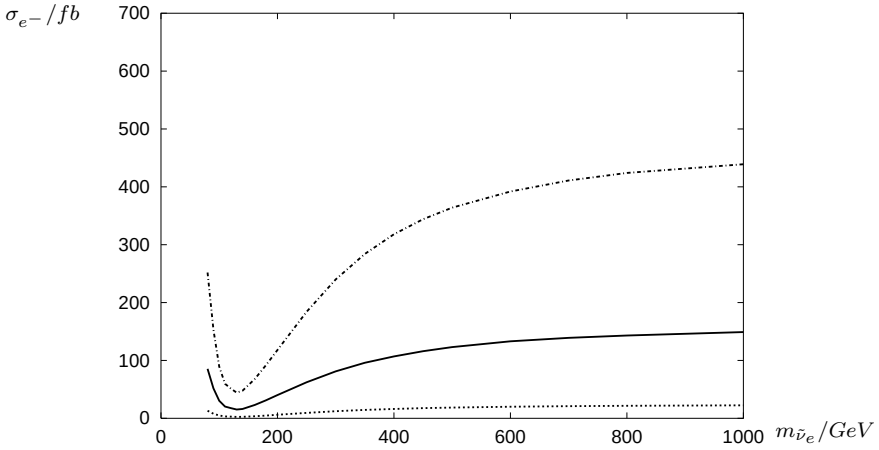

Fig. 1: Cross section σ_{e^-} (see eq. (1)) for $\sqrt{s} = 270$ GeV in scenario A for unpolarized beams (solid line), with only e^- beam polarized $P_- = +85\%$ (dotted line) and with both beams polarized $P_- = -85\%$, $P_+ = +60\%$ (dash-dotted line).

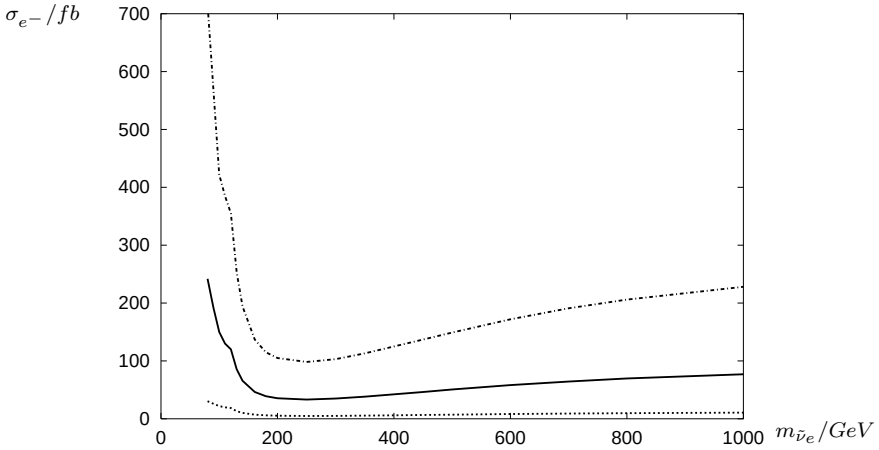

Fig. 2: Cross section σ_{e^-} (see eq. (1)) for $\sqrt{s} = 500$ GeV in scenario A for unpolarized beams (solid line), with only e^- beam polarized $P_- = +85\%$ (dotted line) and with both beams polarized $P_- = -85\%$, $P_+ = +60\%$ (dash-dotted line).

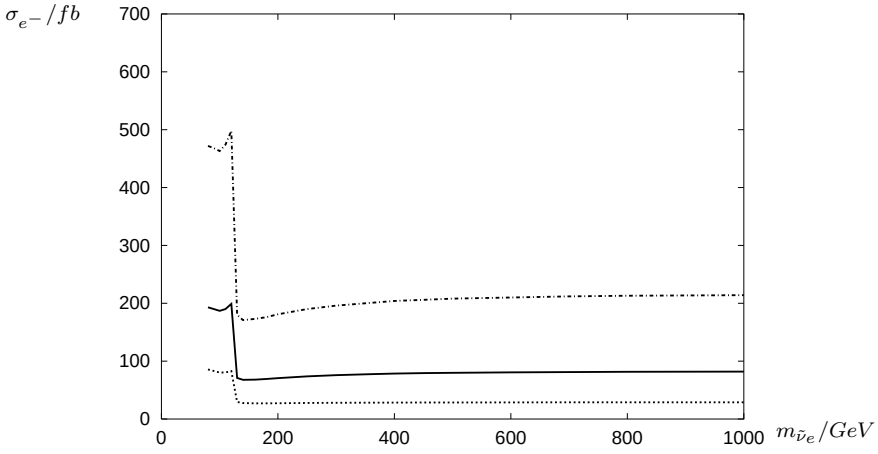

Fig. 3: Cross section σ_{e^-} (see eq. (1)) for $\sqrt{s} = 270$ GeV in scenario B for unpolarized beams (solid line), with only e^- beam polarized $P_- = +85\%$ (dotted line) and with both beams polarized $P_- = -85\%$, $P_+ = +60\%$ (dash-dotted line).

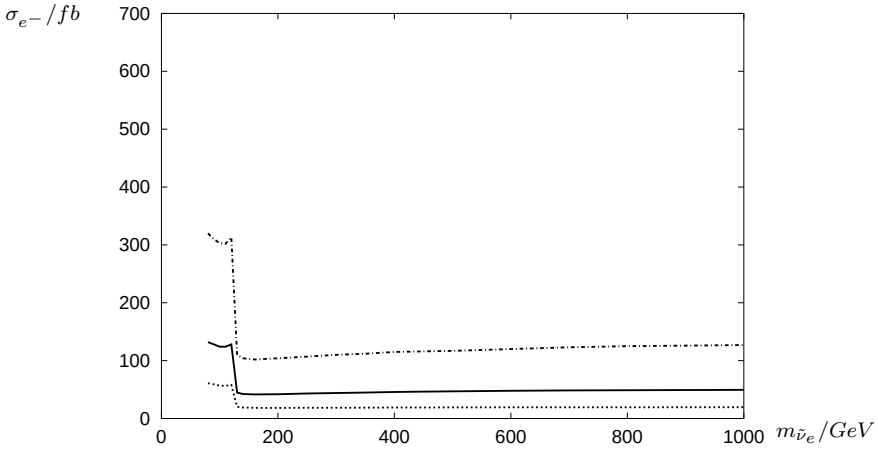

Fig. 4: Cross section σ_{e^-} (see eq. (1)) for $\sqrt{s} = 500$ GeV in scenario B for unpolarized beams (solid line), with only e^- beam polarized $P_- = +85\%$ (dotted line) and with both beams polarized $P_- = -85\%$, $P_+ = +60\%$ (dash-dotted line).

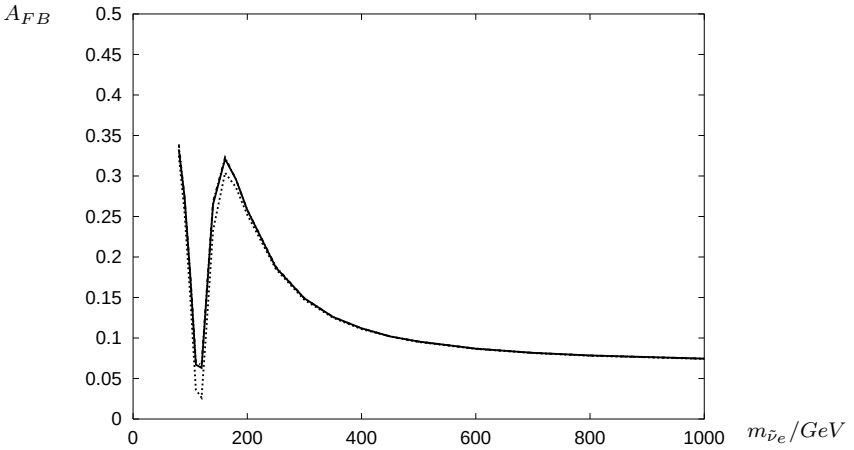

Fig. 5: Electron forward–backward asymmetry A_{FB} (see eq. (2)) in the laboratory system for $\sqrt{s} = 270$ GeV in scenario A for unpolarized beams (solid line), with only e^- beam polarized $P_- = +85\%$ (dotted line) and with both beams polarized $P_- = -85\%$, $P_+ = +60\%$ (dash-dotted line).

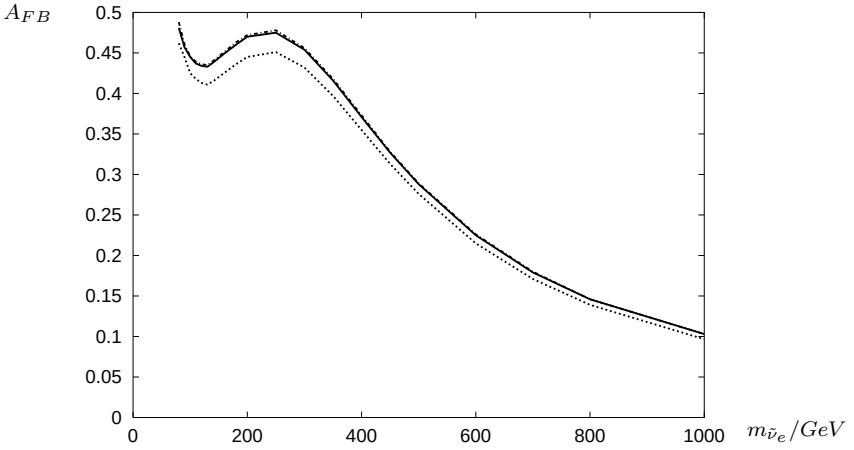

Fig. 6: Electron forward–backward asymmetry A_{FB} (see eq. (2)) in the laboratory system for $\sqrt{s} = 500$ GeV in scenario A for unpolarized beams (solid line), with only e^- beam polarized $P_- = +85\%$ (dotted line) and with both beams polarized $P_- = -85\%$, $P_+ = +60\%$ (dash-dotted line).

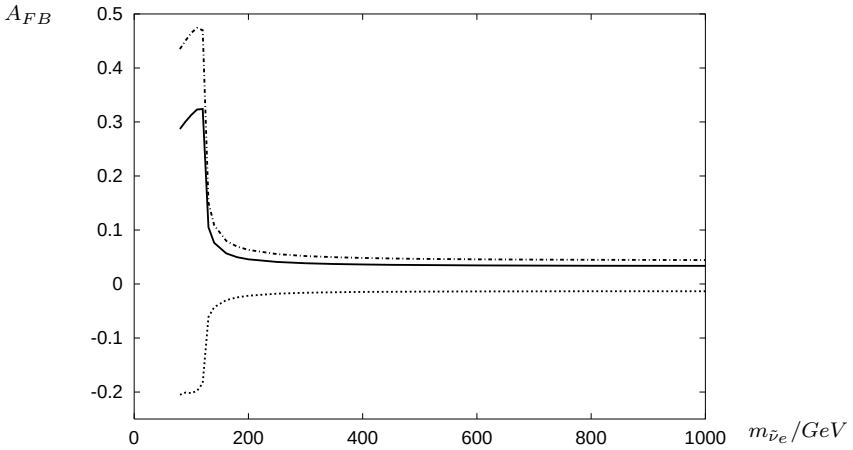

Fig. 7: Lepton forward–backward asymmetry A_{FB} (see eq. (2)) in the laboratory system for $\sqrt{s} = 270$ GeV in scenario B for unpolarized beams (solid line), with only e^- beam polarized $P_- = +85\%$ (dotted line) and with both beams polarized $P_- = -85\%$, $P_+ = +60\%$ (dash-dotted line).

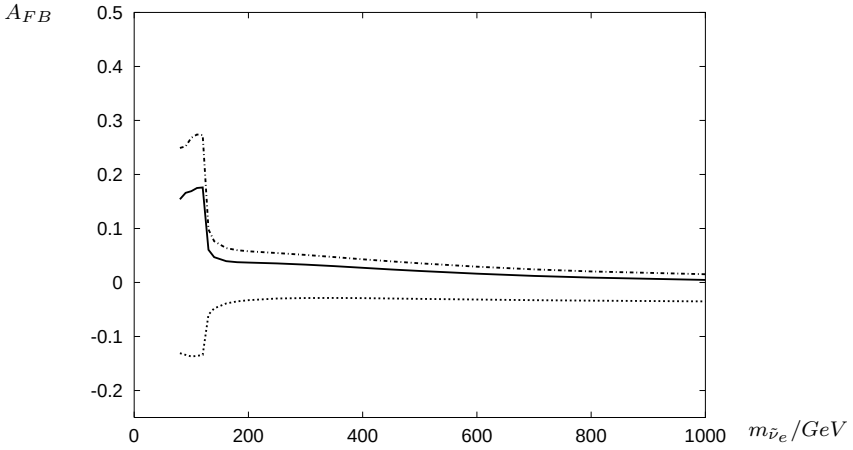

Fig. 8: Lepton forward–backward asymmetry A_{FB} (see eq. (2)) in the laboratory system for $\sqrt{s} = 500$ GeV in scenario B for unpolarized beams (solid line), with only e^- beam polarized $P_- = +85\%$ (dotted line) and with both beams polarized $P_- = -85\%$, $P_+ = +60\%$ (dash-dotted line).